A comparison of discrete curvature schemes applied for triangle meshes derived from geo-spatial data

Mihai-Sorin Stupariu
University of Bucharest

International Conference on Discrete Mathematics:
Discrete Geometry and Convex Bodies
Bucharest, September 2017

Motivation

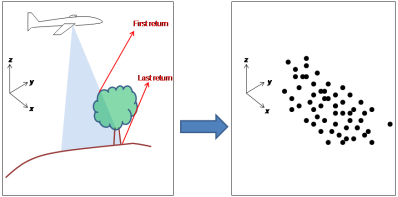

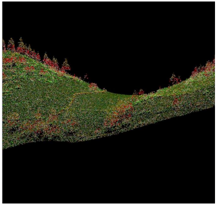

Airborne laser scanning provides a cloud of points situated in the 3D-space (LiDAR data).

Such data sets contain a lot of information useful in practical problems.

Motivation

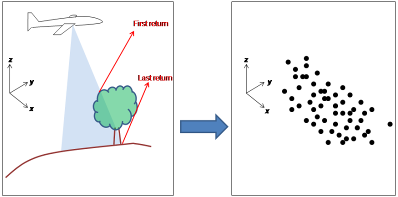

Airborne laser scanning provides a cloud of points situated in the 3D-space (LiDAR data).

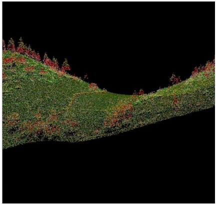

Such data sets contain a lot of information useful in practical problems.

– *Challenge:* explore the opportunity of using tools from Discrete Differential Geometry.

Motivation

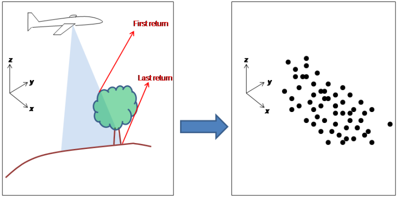

Airborne laser scanning provides a cloud of points situated in the 3D-space (LiDAR data).

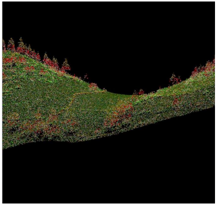

Such data sets contain a lot of information useful in practical problems.

- *Challenge:* explore the opportunity of using tools from Discrete Differential Geometry.
- *Aim:* perform numerical experiments based on true terrain data.

Geo-spatial data - format and representation

Point clouds (LiDAR data)

- rich in information (+)
- appropriate algorithms (+)
- lack of 2D correspondent (–)

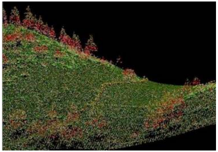

Geo-spatial data - format and representation

Point clouds (LiDAR data)
- rich in information (+)
- appropriate algorithms (+)
- lack of 2D correspondent (–)

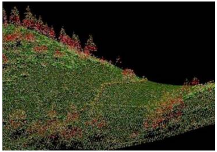

Regularly spaced grids
- easy to handle (+)
- standard patch-corridor model (+)
- lack of details (–)

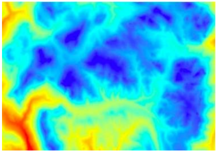

Geo-spatial data - format and representation

Point clouds (LiDAR data)
- rich in information (+)
- appropriate algorithms (+)
- lack of 2D correspondent (–)

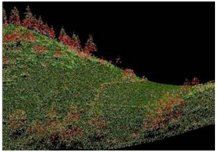

Triangulated terrains (TIN)
- still carry a lot of information (+)
- 2D correspondent possible (+)
- high computational costs (–)

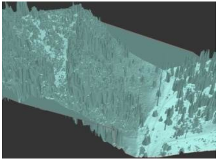

Regularly spaced grids
- easy to handle (+)
- standard patch-corridor model (+)
- lack of details (–)

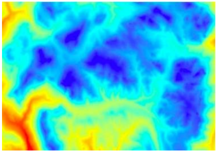

Digital models of the terrain

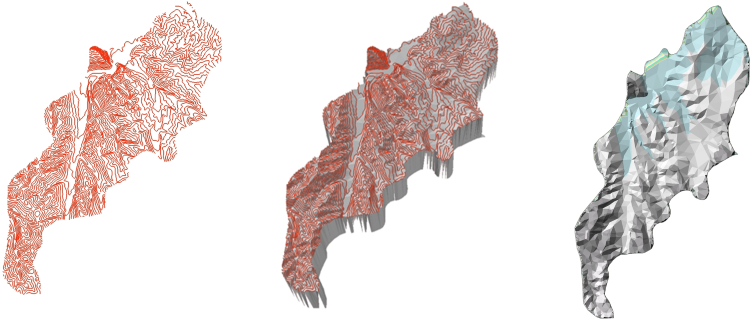

Three representations of the same study site (contour lines, combined, TIN), as provided by GIS-software

TIN representations and terrain variability

- Triangulated terrains in GIS [e.g. de Floriani et al., 1997]

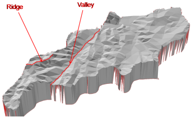

Ridges or valleys are visible in a TIN model

TIN representations and terrain variability

- Triangulated terrains in GIS [e.g. de Floriani et al., 1997]

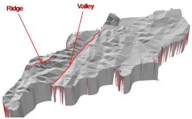

Ridges or valleys are visible in a TIN model

- Recent developments: visibility, computing watersheds [de Berg et al., 2011; de Berg and Tsirogiannis, 2011]

TIN representations and terrain variability

- Triangulated terrains in GIS [e.g. de Floriani et al., 1997]

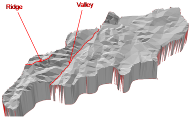

Ridges or valleys are visible in a TIN model

- Recent developments: visibility, computing watersheds [de Berg et al., 2011; de Berg and Tsirogiannis, 2011]
- Main research question: *to what extent is it possible to extract relevant information from geo-spatial data when triangle meshes are used?* Specifically: *how can one measure the lack of flatness?*

TIN representations and terrain variability

- Triangulated terrains in GIS [e.g. de Floriani et al., 1997]

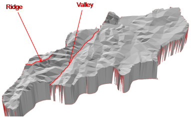

Ridges or valleys are visible in a TIN model

- Recent developments: visibility, computing watersheds [de Berg et al., 2011; de Berg and Tsirogiannis, 2011]
- Main research question: *to what extent is it possible to extract relevant information from geo-spatial data when triangle meshes are used?* Specifically: *how can one measure the lack of flatness?*
- Main hypothesis: *discrete curvatures for triangle meshes could provide relevant numerical descriptors (morphometric variables, e.g. slope, curvatures) quantifying terrain features.* Two tracks: (i) comparisons for various methods; (ii) identification of specfic structures.

Morphometric variables – the discrete approach

Standard approach

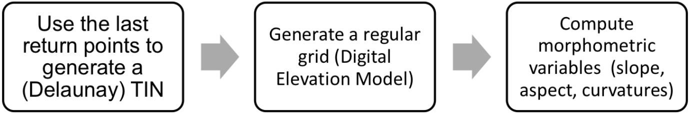

Proposed approach

Notation: 1-ring $\mathcal{N}_{\mathbf{v}}$

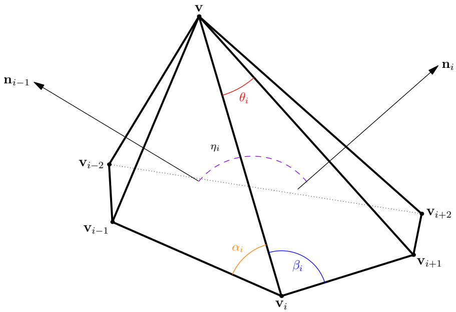

Geometric elements around a vertex $\mathbf{v}$:

Notation: 1-ring $\mathcal{N}_{\mathbf{v}}$

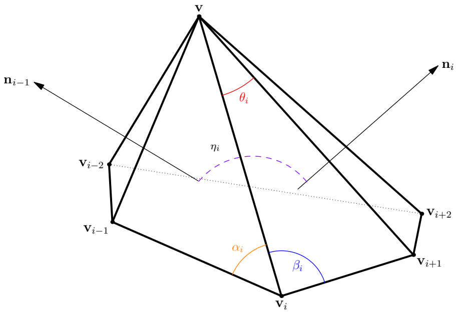

Geometric elements around a vertex $\mathbf{v}$:

- Edges / faces incident to $\mathbf{v}$ (or associated measures – lengths, areas).

Notation: 1-ring $\mathcal{N}_{\mathbf{v}}$

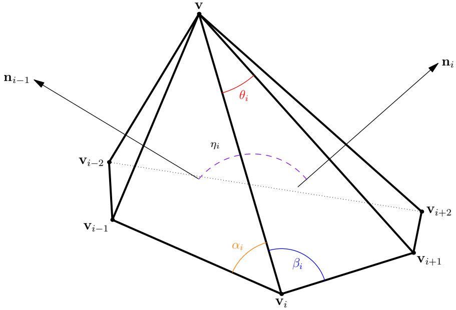

Geometric elements around a vertex $\mathbf{v}$:

- Edges / faces incident to $\mathbf{v}$ (or associated measures – lengths, areas).
- Angles $(\theta_i)_i$ between edges incident to $\mathbf{v}$.

Notation: 1-ring $\mathcal{N}_{\mathbf{v}}$

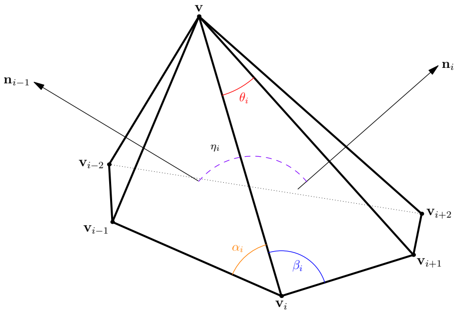

Geometric elements around a vertex **v**:

- Edges / faces incident to **v** (or associated measures – lengths, areas).
- Angles $(\theta_i)_i$ between edges incident to **v**.
- Angles $(\eta_i)_i$ between normals of faces incident to **v**.

Notation: 1-ring $\mathcal{N}_{\mathbf{v}}$

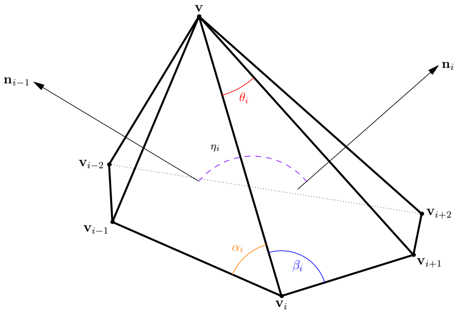

Geometric elements around a vertex **v**:

- Edges / faces incident to **v** (or associated measures – lengths, areas).
- Angles $(\theta_i)_i$ between edges incident to **v**.
- Angles $(\eta_i)_i$ between normals of faces incident to **v**.
- Angles $(\alpha_i)_i, (\beta_i)_i$ between edges of the 1-ring that are not incident to **v**.

Method 1: Gauss-Bonnet scheme (1) GB1

- **Gaussian curvature at v**

$$K_{\mathbf{v}} = \frac{2\pi - \sum_{\mathbf{v}_i \in \mathcal{N}_{\mathbf{v}}} \theta_i}{\frac{1}{3} A}, \tag{1}$$

where $2\pi - \sum_{\mathbf{v}_i \in \mathcal{N}_{\mathbf{v}}} \theta_i$ is the angular defect at **v**, and A is the total area of the triangles in the 1-ring neighborhood of v

Method 1: Gauss-Bonnet scheme (1) GB1

- **Gaussian curvature at v**

$$K_{\mathbf{v}} = \frac{2\pi - \sum_{\mathbf{v}_i \in \mathcal{N}_{\mathbf{v}}} \theta_i}{\frac{1}{3}A}, \tag{1}$$

where $2\pi - \sum_{\mathbf{v}_i \in \mathcal{N}_{\mathbf{v}}} \theta_i$ is the angular defect at **v**, and A is the total area of the triangles in the 1-ring neighborhood of v

- **Mean curvature** at **v**

$$H_{\mathbf{v}} = \frac{\frac{1}{4} \sum_{\mathbf{v}_i \in \mathcal{N}_{\mathbf{v}}} \|\overrightarrow{\mathbf{v}\mathbf{v}_i}\| \eta_i}{\frac{1}{3}A} \tag{2}$$

(measures the variation of the normals along the edges incident to **v**)

Method 1: Gauss-Bonnet scheme (1) GB1

Used by [Dyn et al., 2001]; [Kim et al., 2002] for simplifying triangle meshes

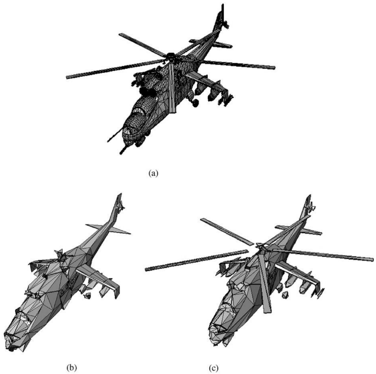

Helicopter model. (a) Original. (b), (c) Simplified versions. In (c) the discrete curvatures were used.
Source: [S.J. Kim, C.H. Kim, D. Levin, *Computers & Graphics*, 2002]

Method 2: Gauss-Bonnet scheme (2) GB2

- Proposed by [Meyer et al., 2003]; considers for averaging A_{mixed} – area of a region determined by circumcenters instead of barycenters (adapted for obtuse triangulations).
- **Gaussian curvature** at **v**

$$K_{\mathbf{v}} = \frac{2\pi - \sum_{\mathbf{v}_i \in \mathcal{N}_{\mathbf{v}}} \theta_i}{A_{\mathrm{mixed}}}. \tag{3}$$

Each triangle of $\mathcal{N}_{\mathbf{v}}$ "contributes" to A_{mixed}. If $\Delta \mathbf{v}\mathbf{v}_{i-1}\mathbf{v}_i$, is non-obtuse, its contribution is $\frac{1}{8}(\|\overrightarrow{\mathbf{v}\mathbf{v}_i}\|^2 \cot(\widehat{\mathbf{v}\mathbf{v}_{i-1}\mathbf{v}_i}) + \|\overrightarrow{\mathbf{v}\mathbf{v}_{i-1}}\|^2 \cot(\widehat{\mathbf{v}\mathbf{v}_i\mathbf{v}_{i-1}}))$. If $\Delta$is obtuse: (i) at **v**: $\frac{1}{2}A(\Delta)$, (ii) at a vertex different of **v**: $\frac{1}{4}A(\Delta)$.

Method 2: Gauss-Bonnet scheme (2) GB2

- Proposed by [Meyer et al., 2003]; considers for averaging A_{mixed} − area of a region determined by circumcenters instead of barycenters (adapted for obtuse triangulations).
- **Gaussian curvature** at **v**

$$K_{\mathbf{v}} = \frac{2\pi - \sum_{\mathbf{v}_i \in \mathcal{N}_{\mathbf{v}}} \theta_i}{A_{\mathrm{mixed}}}. \tag{3}$$

Each triangle of $\mathcal{N}_{\mathbf{v}}$ "contributes" to A_{mixed}. If $\Delta \mathbf{v}\mathbf{v}_{i-1}\mathbf{v}_i$, is non-obtuse, its contribution is $\frac{1}{8}(\|\overrightarrow{\mathbf{v}\mathbf{v}_i}\|^2 \cot(\widehat{\mathbf{v}\mathbf{v}_{i-1}\mathbf{v}_i}) + \|\overrightarrow{\mathbf{v}\mathbf{v}_{i-1}}\|^2 \cot(\widehat{\mathbf{v}\mathbf{v}_i\mathbf{v}_{i-1}}))$. If $\Delta$is obtuse: (i) at **v**: $\frac{1}{2}A(\Delta)$, (ii) at a vertex different of **v**: $\frac{1}{4}A(\Delta)$.

- **The mean curvature** $H_{\mathbf{v}} = \frac{1}{2}\|\mathbf{H}_{\mathbf{v}}\|$ is the norm of the mean curvature operator

$$\mathbf{H}_{\mathbf{v}} = \frac{1}{2A_{\mathrm{mixed}}} \sum_{\mathbf{v}_i \in \mathcal{N}_{\mathbf{v}}} (\cot(\widehat{\mathbf{v}\mathbf{v}_{i-1}\mathbf{v}_i}) + \cot(\widehat{\mathbf{v}\mathbf{v}_{i+1}\mathbf{v}_i}))\overrightarrow{\mathbf{v}_i\mathbf{v}}. \tag{4}$$

Method 3: approach based on Euler's theorem ET

- Proposed by [Watanabe & Belyaev, 2001], based on integral formulas derived from Euler's theorem

$$H = \frac{1}{2\pi}\int_0^{2\pi} \kappa_\nu(\varphi) d\varphi; \qquad K = 3H^2 - \frac{1}{\pi}\int_0^{2\pi} \kappa_\nu(\varphi)^2 d\varphi,$$

$\kappa_\nu(\varphi)$ is the normal curvature of the normal section curve corresponding to the angle φ.

Method 3: approach based on Euler's theorem ET

- Proposed by [Watanabe & Belyaev, 2001], based on integral formulas derived from Euler's theorem

$$H = \frac{1}{2\pi}\int_0^{2\pi} \kappa_\nu(\varphi)d\varphi; \qquad K = 3H^2 - \frac{1}{\pi}\int_0^{2\pi} \kappa_\nu(\varphi)^2 d\varphi,$$

$\kappa_\nu(\varphi)$ is the normal curvature of the normal section curve corresponding to the angle φ.

- Approximate $\kappa_\nu(\varphi)$ along the edges of the 1-ring by

$$\kappa_{\nu,i} \simeq \frac{2 < \mathbf{n}_v, \overrightarrow{vv_i} >}{\| \overrightarrow{vv_i} \|^2} \tag{5}$$

($\mathbf{n}_v$ weighted normal; weights are relative areas).

- Use approximation and put

$$H_v = \frac{1}{2\pi}\sum_{i=1}^{n} \kappa_{\nu,i}\frac{\theta_{(i-1) \bmod n} + \theta_i}{2}; \quad K_v = 3H_v^2 - \frac{1}{\pi}\sum_{i=1}^{n} \kappa_{\nu,i}^2\frac{\theta_{(i-1) \bmod n} + \theta_i}{2}$$

Method 4: the tensor approach TA

- Proposed by [Taubin, 1995]
- Define the normal curvature $\kappa_{\nu,i}$ along the edge $\overrightarrow{\mathbf{vv}_i}$ as in (5).

Method 4: the tensor approach TA

- Proposed by [Taubin, 1995]
- Define the normal curvature $\kappa_{\nu,i}$ along the edge $\overrightarrow{\mathbf{v}\mathbf{v}_i}$ as in (5).
- Approximate the corrsponding tangent vector by normalizing the projecton of $\overrightarrow{\mathbf{v}\mathbf{v}_i}$ onto the plane orthogonal to $\overrightarrow{\mathbf{n}}_{\mathbf{v}}$, that is $\overrightarrow{\mathbf{t}}_i = \frac{(\mathbb{I}_3 - \overrightarrow{\mathbf{n}}_v \overrightarrow{\mathbf{n}}_v^t)(\mathbf{v}_i - \mathbf{v})}{\|(\mathbb{I}_3 - \overrightarrow{\mathbf{n}}_v \overrightarrow{\mathbf{n}}_v^t)(\mathbf{v}_i - \mathbf{v})\|}$.

Method 4: the tensor approach TA

- Proposed by [Taubin, 1995]
- Define the normal curvature $\kappa_{\nu,i}$ along the edge $\overrightarrow{\mathbf{vv}_i}$ as in (5).
- Approximate the corrsponding tangent vector by normalizing the projecton of $\overrightarrow{\mathbf{vv}_i}$ onto the plane orthogonal to $\overrightarrow{\mathbf{n}}_{\mathbf{v}}$, that is $\overrightarrow{\mathbf{t}}_i = \frac{(\mathbb{I}_3 - \overrightarrow{\mathbf{n}}_v \overrightarrow{\mathbf{n}}_v^t)(\mathbf{v}_i - \mathbf{v})}{\|(\mathbb{I}_3 - \overrightarrow{\mathbf{n}}_v \overrightarrow{\mathbf{n}}_v^t)(\mathbf{v}_i - \mathbf{v})\|}$.
- Define the matrix $M_{\mathbf{v}}$ as a weighted sum, $M_{\mathbf{v}} = \sum_{i=1}^{d_{\mathbf{v}}} \rho_i \kappa_{\nu,i} \overrightarrow{\mathbf{t}}_i \overrightarrow{\mathbf{t}}_i^t$, where the weight ρ_i the relative area of the faces that are adjacent to the edge $\overrightarrow{\mathbf{vv}_i}$.

Method 4: the tensor approach TA

- Proposed by [Taubin, 1995]
- Define the normal curvature $\kappa_{\nu,i}$ along the edge $\overrightarrow{\mathbf{vv}_i}$ as in (5).
- Approximate the corrsponding tangent vector by normalizing the projecton of $\overrightarrow{\mathbf{vv}_i}$ onto the plane orthogonal to $\overrightarrow{\mathbf{n}}_{\mathbf{v}}$, that is $\overrightarrow{\mathbf{t}}_i = \frac{(\mathbb{I}_3 - \overrightarrow{\mathbf{n}}_v \overrightarrow{\mathbf{n}}_v^t)(\mathbf{v}_i - \mathbf{v})}{\|(\mathbb{I}_3 - \overrightarrow{\mathbf{n}}_v \overrightarrow{\mathbf{n}}_v^t)(\mathbf{v}_i - \mathbf{v})\|}$.
- Define the matrix $M_{\mathbf{v}}$ as a weighted sum, $M_{\mathbf{v}} = \sum_{i=1}^{d_{\mathbf{v}}} \rho_i \kappa_{\nu,i} \overrightarrow{\mathbf{t}}_i \overrightarrow{\mathbf{t}}_i^t$, where the weight ρ_i the relative area of the faces that are adjacent to the edge $\overrightarrow{\mathbf{vv}_i}$.
- By the construction of $M_{\mathbf{v}}$, one of its eigenvalues is 0, with associated eigenvector $\overrightarrow{\mathbf{n}}_{\mathbf{v}}$. Let λ and μ be the other eigenvalues of $M_{\mathbf{v}}$. Put

$$K_{\mathbf{v}} = (3\lambda - \mu) \cdot (3\mu - \lambda); \qquad H_{\mathbf{v}} = \frac{1}{2}\left[(3\lambda - \mu) + (3\mu - \lambda)\right].$$

Method 5: paraboloid fitting PF

Assume that $v = 0$ and $\mathbf{n_v} = (0,0,1)$; take its 1-ring neighborhood and find a paraboloid $z = ax^2 + bxy + cy^2$ that better fits this data (using least squares fitting, e.g. [Hamann, 1993]); then compute K_v, H_v by using standard formulas for the smooth paraboloid

$$K_{\mathbf{v}} = 4ac - b^2; \qquad H_{\mathbf{v}} = a + c. \tag{6}$$

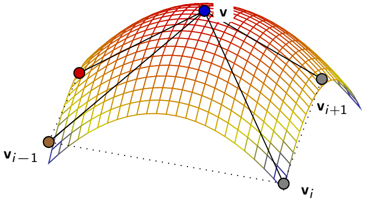

Method 6: Shape Operator SO

- Proposed by [Hildebrandt & Polthier, 2004]
- One defines the *mean curvature for an edge e*
  $H_e = 2\|e\| \cos \frac{\eta_e}{2}$.

Method 6: Shape Operator SO

- Proposed by [Hildebrandt & Polthier, 2004]
- One defines the *mean curvature for an edge e* $H_e = 2\|e\| \cos \frac{\eta_e}{2}$.
- The *Shape Operator* at the vertex **v**

$$S(\mathbf{v}) = \frac{1}{2} \sum_{e_i \in \mathcal{N}_{\mathbf{v}}} \omega_{e_i} H_{e_i} \; \vec{t}_{e_i} \vec{t}_{e_i}^{\,t},$$

where $\omega_e = \langle \mathbf{n_v}, \mathbf{n}_e \rangle$, and $\vec{t}_e$ is the versor of the projection on the "tangent" plane at **v** of the vector $\vec{e} \times \vec{\mathbf{n}}_e$.

Method 6: Shape Operator SO

- Proposed by [Hildebrandt & Polthier, 2004]
- One defines the *mean curvature for an edge e* $H_e = 2\|e\| \cos \frac{\eta_e}{2}$.
- The *Shape Operator* at the vertex $\mathbf{v}$

$$S(\mathbf{v}) = \frac{1}{2} \sum_{e_i \in \mathcal{N}_{\mathbf{v}}} \omega_{e_i} H_{e_i} \overrightarrow{t}_{e_i} \overrightarrow{t}_{e_i}^{\,t},$$

where $\omega_e = \langle \mathbf{n_v}, \mathbf{n}_e \rangle$, and $\overrightarrow{t}_e$ is the versor of the projection on the "tangent" plane at $\mathbf{v}$ of the vector $\overrightarrow{e} \times \overrightarrow{\mathbf{n}}_e$.

- The Gaussian curvature and the mean curvature, respectively, are defined by

$$K_{\mathbf{v}} = \det(S(\mathbf{v})); \; H_{\mathbf{v}} = \frac{1}{2}\mathrm{tr}(S(\mathbf{v})). \tag{7}$$

Concept

- Comparisons between the methods: realized for surfaces such as plane, sphere, cone, cylinder [Magid, Soldea, Rivlin, 2007].

Concept

- Comparisons between the methods: realized for surfaces such as plane, sphere, cone, cylinder [Magid, Soldea, Rivlin, 2007].
- **Aim:** computation and comparisons for geo-spatial data, obtained thrhough *in situ* measurements – true terrains, with unknown geometry of the underlying surface.

Concept

- Comparisons between the methods: realized for surfaces such as plane, sphere, cone, cylinder [Magid, Soldea, Rivlin, 2007].
- **Aim:** computation and comparisons for geo-spatial data, obtained thrhough *in situ* measurements – true terrains, with unknown geometry of the underlying surface.
- Two complementary approaches: refining and coarsening.

Approach 1 - approximation accuracy

- Generate a discrete height function starting from the elevation digital model of a site situated in a mountainous region (cca. 23 km^2).

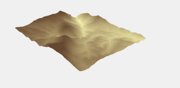

- Produce a smooth surface S by standard interpolation techniques.
- Select on S, through jittered sampling with decreasing cell size (i.e., increasing resolution), sets of random points ('pseudo-LiDAR data sets'). Four cell sizes were used throughout the experiments having a size equal to a ratio of 1, 0.5, 0.25 and 0.125 to the original cell size. These values correspond to real cell sizes of 18 m, 9 m, 4.5 m and 2.25 m, respectively.
- Generate a 2.5D triangular irregular network for each point set, obtained for each of the four levels of resolution.
- Compare the discrete Gaussian curvature and discrete mean curvature with the 'true' smooth ones. For each method, at each of the four levels of resolution, two numerical quantities were computed: (i) the absolute error (normalized L^1-norm of the vector of differences between 'discrete' and 'smooth' curvatures); (ii) the correlation coefficients between the discrete and the smooth curvatures.

Results (1): Gaussian curvature

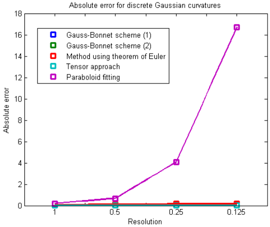

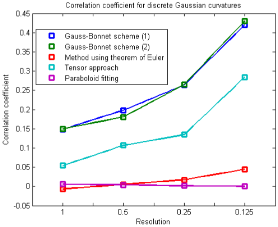

– In the computation of the absolute error and of the correlation coefficient all points are taken into account
– **Gauss-Bonnet scheme**: best approximation
– **Paraboloid fitting**: bad behavior (occurrence of outliers)
– Hierarchy is similar for spline interpolation
– The results for SO-method are not included in the diagrams

Results (1): Gaussian curvature - outliers removed

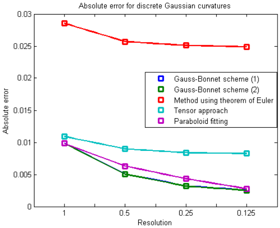

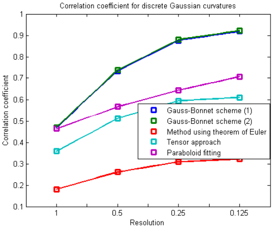

– In the computation of the absolute error and of the correlation coefficient the 'outliers' were removed
– **Gauss-Bonnet scheme**: best approximation
– **Paraboloid fitting**: sensitive to occurrence of outliers

Results (1): mean curvature

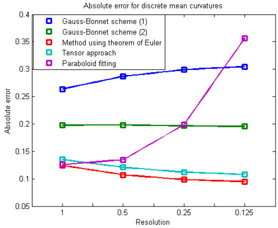

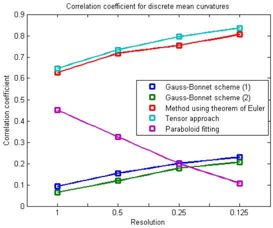

– In the computation of the absolute error and of the correlation coefficient all points are taken into account

– **Method using Euler's theorem and the tensor approach**: best approximation

– **Paraboloid fitting**: bad behavior

– Hierarchy is similar for spline interpolation

– The results for SO-method are not included in the diagrams

Results (1): mean curvature - outliers removed

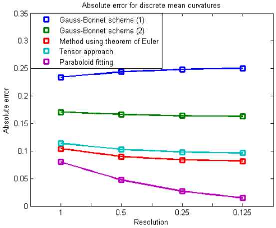

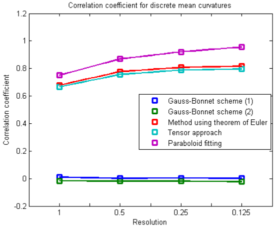

– In the computation of the absolute error and of the correlation coefficient 'outliers' are removed

– **Method using Euler's theorem**: good approximation / not sensitive to outliers

– **Paraboloid fitting**: best approximation / sensitive to occurrence of outliers

Approach 2 - smoothening

- Numerical experiments based on true terrain data: high resolution point cloud of size 427K; surface of cca. 2.5 ha.
- Preprocess data: crop and a rectangle having sizes 128 m and 160 m.
- For cell sizes equal to 0.5 m, 1 m, 2 m, 4 m, 8 m, 16 m, regularly spaced grids were generated. For each cell $\mathcal{C}$, a single point was obtained, by averaging the coordinates of the points of the original cloud situated in $\mathcal{C}$.
- For each point set, obtained for each of the six levels of resolution, a 2.5D Delaunay triangulation was generated.
- The values of the discrete Gaussian and mean curvatures for the vertices of each set and for the corresponding regularly spaced grids were computed. For each method, the discrete Gaussian curvature and discrete mean curvature were compared with the ones computed for the corresponding regular grids. The comparison was achieved by computing two numerical quantities: (i) the absolute error (normalized L^1-norm of the difference vectors), (ii) the correlation coefficients. For a better relevance, border vertices or vertices for which some of the methods could not provide any value were removed from the statistics.

Results (2): Gaussian curvature

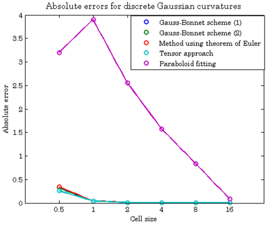

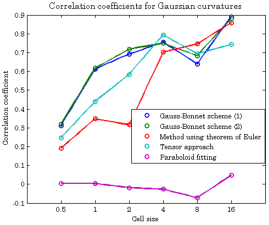

– Absolute error and correlation coefficients: GB1, GB2, ET, TA comparable results (smoothening effect).

– The results for SO-method are not included in the diagrams

Results (2): mean curvature

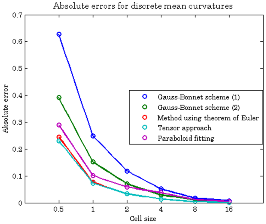

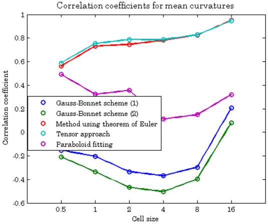

– **Method using Euler's theorem and the tensor approach**: best approximation

– Weak correlations for GB1, GB2 (only positive values).

Conclusions

For the **Gaussian curvature**, the best approximation was given by the Gauss-Bonnet schemes, while in the case of the **mean curvature**, the tensor approach and the method based on Euler's theorem provided an accurate estimate. These findings are consistent for both approaches and they are consistent with previous studies conducted for smooth surfaces with known underlying geometry.

Problem statement

Vegetation structures (e.g. trees) are visible in a high density point cloud and in the associated triangulation.

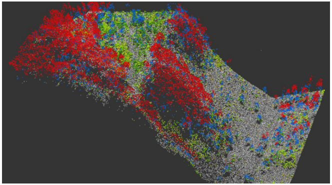

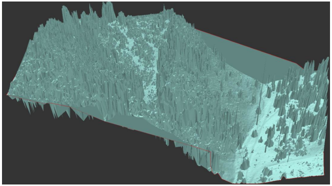

Methodology

- The high resolution LiDAR point cloud was used; a 2.5 Delaunay triangulation was generated direclty from the original point cloud ((x, y)-duplicates, due to vegetation, were eliminated).

Methodology

- The high resolution LiDAR point cloud was used; a 2.5 Delaunay triangulation was generated direclty from the original point cloud ((x, y)-duplicates, due to vegetation, were eliminated).
- Compute the values of discrete curvatures for the triangle mesh associated to the original point cloud. For each discrete curvature get a grid of averaged curvatures (cell size 1m).

Methodology

- The high resolution LiDAR point cloud was used; a 2.5 Delaunay triangulation was generated direclty from the original point cloud ((x, y)-duplicates, due to vegetation, were eliminated).
- Compute the values of discrete curvatures for the triangle mesh associated to the original point cloud. For each discrete curvature get a grid of averaged curvatures (cell size 1m).
- Construct regular grids (cell size 1m) of curvatures. Construirea unor “grile regulate de curburi”, având celula cu dimensiunea de 1m. For each method and cell one considered the vertices lying in that cell and then one computed the average value of the curvatures corresponding to these vertices.

Methodology

- The high resolution LiDAR point cloud was used; a 2.5 Delaunay triangulation was generated direclty from the original point cloud ((x, y)-duplicates, due to vegetation, were eliminated).
- Compute the values of discrete curvatures for the triangle mesh associated to the original point cloud. For each discrete curvature get a grid of averaged curvatures (cell size 1m).
- Construct regular grids (cell size 1m) of curvatures. Construirea unor "grile regulate de curburi", având celula cu dimensiunea de 1m. For each method and cell one considered the vertices lying in that cell and then one computed the average value of the curvatures corresponding to these vertices.
- Use pattern recognition techniques (the Hough transform, implemented in Matlab, sensitivity factor 0.85) for detecting circles: horizontal projections of tree crowns usually yield circular shapes.

Tree detection – results

LiDAR point cloud (colours represent height above ground, in particular trees are coloured in red).

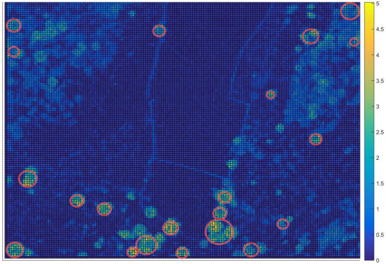

Grid generated by using the mean curvature, as provided by the shape operator method. The red circles represent

Tree detection – results

The point cloud (3D representation).

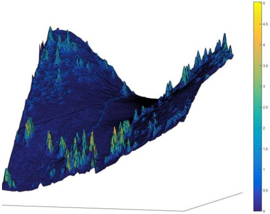

Grid of mean curvatures for SO (3D representation).

Comparisons – mean curvature grids

Point cloud.

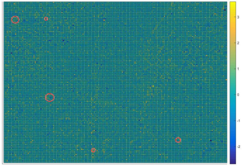

ET

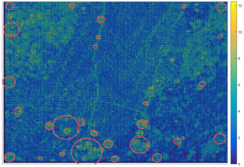

GB1

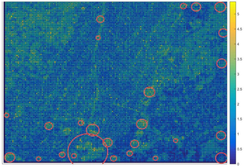

GB2

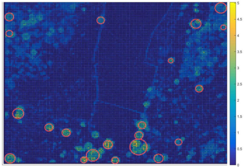

SO

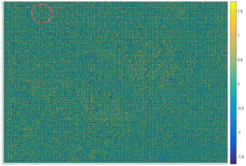

TA

Comments and conclusions

- Mean curvature - makes it possible to detect trees and the size of their crowns.
- Good results for SO; similar results for GB1, GB2.
- Advantages:
    - The method presented is independent on any *a priori* knowledge, while state of the art techniques require a preliminary field survey, enabling an appropriate calibration and developing suitable regression models, (e.g. [Popescu, 2003]).
    - Independence on tree species, while other approaches are species sensitive: [Falkowski et al., 2006] an aaproach on the Mexican Hat wavelet appropriate for coniferous trees.

References

M.J. Falkowski, A.M.S. Smith, A.T. Hudak et al., Automated estimation of individual conifer tree height and crown diameter via two-dimensional spatial wavelet analysis of lidar data, *Canadian Journal of Remote Sensing*, **32** (2006), 153–161.

L. de Floriani, E. Puppo, P. Magillo (1997) *Applications of Computational Geometry to Geographical Information Systems*

B. Hamann, Curvature approximation for triangulated surfaces, *Computing Suppl.*, **8** (1993) 139-153.

K. Hildebrandt, K. Polthier, Anisotropic Filtering of Non-Linear Surface Features, *Computer Graphics Forum*, **23** (2004), 391–400.

S.J. Kim, C.H. Kim, D. Levin, Surface simplification using a discrete curvature norm, *Computers & Graphics*, **26** (2002), 657-663.

E. Magid, O. Soldea, E. Rivlin (2007) A comparison of Gaussian and mean curvature estimation methods on triangular meshes of range image data. *Computer Vision and Image Understanding* **107** 139-159.

M. Meyer, M. Desbrun, P. Schröder, A. Barr (2003) Discrete differential-geometry operators for triangulated 2-manifolds, in: H.C. Hege, K. Polthier (Eds.), *Visualization and Mathematics III*, 35-57.

S.C. Popescu, R.H. Wynne, R.F. Nelson, Measuring individual tree crown diameter with lidar and assessing its influence on estimating forest volume and biomass, *Canadian Journal of Remote Sensing*, **29** (2003), 564–577.

P. Shary, L. Sharaya, A. Mitusov (2002) Fundamental quantitative methods of land surface analysis. *Geoderma* **1**, 1-32.

G. Taubin, Estimating the tensor of curvature of a surface from a polyhedral approximation, in *The Fifth International Conference on Computer Vision*, 1995, pp. 902–907.

K. Watanabe, A.G. Belyaev, Detection of salient curvature features on polygonal surfaces, in: *Eurographics 2001*, vol. 20, No. 3, 2001.

Thank you!